Arabian Journal of Chemical and Environmental Research

Vol. 08 Issue 2 (2021) 336–354

Performance of 5-amino-1,3,4-thiadiazole-2-thiol as corrosion inhibitor for aluminium in dilute hydrochloric acid medium

U. Yunusa[1*], A. I. Kubo[2], G. N. Bello[3], and A. Shehu[4]

[1] *Department of Pure and Industrial Chemistry, Faculty of Physical Sciences, Bayero University, Kano, Nigeria.*
[2] *Department of Pure and Applied Chemistry, Adamawa State University, Mubi, Nigeria.*
[3] *Chemical Division, Industrial Development Department, FMITI, PMB 88, Garki 1, Abuja, Nigeria.*
[4] *Department of General Studies, Federal College of Agricultural Produce Technology, Kano, Nigeria.*

Received 10 June 2021, Revised 23 Oct 2021, Accepted 23 Oct 2021

Abstract

The inhibition performance of 5-amino-1,3,4-thiadiazole-2-thiol (5-ATT) on aluminium corrosion in acidic medium was investigated using experimental and theoretical approach. The weight loss measurements demonstrated that the inhibition efficiency increased with an increase in concentration of 5-ATT but decreased at elevated temperatures. The inhibitor molecule exhibited the highest inhibition efficiency of 94.28 % at 2.0 mM for T = 308 K. The adsorption of the 5-ATT on aluminium surface in acid solution was found to obey the Langmuir isotherm and the value of ΔG^{o}_{ads} suggest a combination of both physisorption and chemisorption mechanisms. Scanning electron microscopy analysis demonstrated the adsorption of 5-ATT on the aluminium surface which justified the observed anticorrosion activity. Besides, the correlation between inhibition performance and the electronic structure parameters of the inhibitor was theoretically elucidated via quantum chemical calculations. Molecular dynamics simulations were engaged to provide insights into the mechanism of interaction between the inhibitor and the aluminium surface. The theoretical outcomes highlighted the ability of the 5-ATT to adsorbed favourably on the Al (1 1 0) surface in parallel orientation.

Keywords: 1,3,4-thiadiazole, Aluminium, Corrosion inhibition, Quantum chemical calculations, MD simulations.

*Corresponding author.
E-mail address: umaryunusa93@gmail.com

1. Introduction

Corrosion protection of metallic materials has been a subject of intense research due to huge economic and safety misfortunes as a result of corrosion in various industries. The corrosion can cause a substantial loss of energy and contributes to environmental degradation [1]. Aluminum and its alloys are among the most widely used materials because of their lightness, oxidation resistance, low cost, high electrical capacity and prevailing mechanical strength. They are employed in various industries, especially the marine, electronics, aerospace, constructions, household and food industry [2,3]. Nowadays, hydrochloric acid solutions are heavily used in industries, mainly in acid stripping of aluminium, industrial cleaning, pickling and descaling [4,5]. There is, however, a major risk to use acid solutions because aluminium is aggressively attacked by acid solutions which affects the integrity of the metal surface. In aqueous solution, aluminium exhibit excellent corrosive resistance owing to its ability to form a stable thin oxide film on its surface which protect it from the corrosion phenomenon. However, this film has an amphoteric receptivity and substantially dissolves when aluminium is in contact with aggressive media such as HCl [6]. The chloride ions of the acid have the ability to initiate pitting corrosion at vulnerable sites of the film-protected metal. Consequently, it is necessary to discover effective methods to safeguard aluminium from corrosion in acidic media and avert the allied economic losses.

Several approaches have been described in literature for the protection of metals against corrosion in aggressive media. The use of organic compounds containing heteroatoms such as P, N, O and S, polar functional groups and conjugate system as corrosion inhibitors is one of the most popular, cost-effective and practical strategies for mitigating corrosion in acidic solutions or other corrosive environment [7,8]. The inhibitive properties of most organic molecules is often ascribed to their adsorption capability on the metal surface, which hampers the corrosion reactions occurring on metal surface, thereby protecting the metal and increasing the life span. Recently, due to stringent environmental regulation, the choice of corrosion inhibitors has been geared towards the use of inhibitors that are less toxic, biodegradable, inexpensive and ecologically friendly [9,10]. In this regard, heterocyclic compounds are widely used for corrosion inhibition in acidic media because of their low toxicity and excellent adsorption characteristics [11].

According to literature, only a few studies have been conducted regarding the corrosion inhibition efficacy of 5-amino-1,3,4-thiadiazole-2-thiol on metals in aggressive media [12,13]. To the authors' best knowledge, no report has been documented so far on the anticorrosive effect of this compound towards the corrosion of aluminium in acidic medium. Hence, the inhibitive properties of 5-amino-1,3,4-thiadiazole-2-thiol on aluminium corrosion in 1 M HCl solution was investigated by employing both

experimental and theoretical approaches. The inhibition performance of the target inhibitor was assessed using weight loss analysis. Additionally, both quantum chemical computations and molecular dynamics simulation were further engaged to explore the adsorption properties of the inhibitor on aluminium surface.

2. Experimental details

2.1. Materials and solutions

Aluminum sheet of chemical composition (wt%): Al (99.50), Fe (0.3202), Si (0.0085), Ti (0.0074), Zn (0.0060), Ni (0.0045), Cr (0.0041), Mn (0.0030), Sn (0.0024), Mg (0.0018), Cu (0.0015) and Pb (0.0007) was employed as test material for all weight loss experiments. The aluminium sample was cut into specimens of dimension 2.5 cm × 2.5 cm × 0.3 cm. Prior to each anticorrosion test, the surfaces of the aluminium specimens were mechanically abraded with SiC emery papers of different grit sizes (600-1200). After that, the polished surface was cleaned with bi-distilled water, degreased with acetone (99.5%), washed with absolute ethanol and finally dried with a clean towel paper. The aluminium specimens were used for corrosion test immediately after surface preparation. The aggressive medium of 1 M HCl was prepared from 37% analytical grade HCl using bi-distilled water. The 5-amino 1,3,4-thiadiazole-2-thiol (5-ATT) employed as corrosion inhibitor in the present study has been applied at concentrations ranging from 0.1 to 2.0 mM. The chemical structure of 5-ATT is displayed in **Fig. 1.**

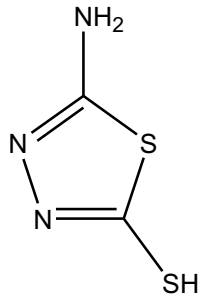

Fig. 1. Chemical structure of 5-amino-1,3,4-thiadiazole-2-thiol (5-ATT).

2.2. Weight loss experiment

Aluminium specimens with the previously stated chemical compositions and dimensions 2.5 cm× 2.5 cm× 0.3 cm were used for all weight loss measurements. The initial weights of the thoroughly polished specimens were recorded before immersion in the test solution. The experiments were performed in a thermostatically controlled water bath with the specimens immersed into beakers containing 1 M HCl (100 mL) corrosive solutions one without the 5-ATT inhibitor (blank), and the others with varying concentrations of 5-ATT (0.1–2.0 mM) for 6 hours and at different temperatures (308─338 K). Afterwards, the specimens were retrieved from the corrosive solutions, cleaned appropriately until the

corrosion products on the specimens' surface were removed, then dried and finally reweighed. Weight loss tests were likewise carried out at different time, that is, 3, 6, 9 and 12 h to analyze the influence of immersion time on the corrosion phenomenon. The loss in weight of specimen was computed which is basically the weight difference of the Al specimens before and after immersion in the acidic solution. All the experiments were run in triplicate to ensure reproducibility, and the average values were reported in each case.

The corrosion rates (C_R; mg. cm^{-2} h^{-1}) and inhibition efficiency (IE; %) were determined from the weight loss data as per eqs 1 and 2 [14]:

$$C_R = \frac{W_1 - W_2}{At} \qquad (1)$$

$$IE\ (\%) = \frac{C_R^0 - C_R^i}{C_R^o} \times 100 \qquad (2)$$

where W_1 and W_2 represent the weight (mg) of aluminium specimen before and after immersion in the test solution; A signifies the exposed area of aluminum specimen (cm^2); t is the immersion time (h); C_R^o and C_R^i represent the corrosion rate (mg. cm^{-2} h^{-1}) in the absence and presence of 5-ATT inhibitor, respectively.

2.3. Computational quantum studies

Quantum chemical calculations were carried out using DMol^3 module under DFT approximation of a Materials Studio software (version 8.0). The molecular structure of the tested inhibitor was sketched using ChemDraw Ultra 7.0 software. DFT calculations at the Becke's three-parameter hybrid functional with the LYP correlation functional (B3LYP) using a double numerical basis set (DND) were performed to explore the electronic properties of the tested molecule. After the geometry optimization step, the electronic density distributions (HOMO, LUMO) and some relevant quantum chemical indexes, i.e., energy of HOMO (E_{HOMO}), energy of the LUMO (E_{LUMO}), energy gap ($\Delta E = E_{LUMO} - E_{HOMO}$), ionization energy (I), electronic affinity (A), chemical hardness (η), softness (S), global electronegativity (χ), chemical potential (μ) and electrophilicity index (ω) of the molecule were estimated and discussed. Other parameters describing the local selectivity of the 5-ATT molecule such as the condensed Fukui functions and the dual descriptor are also considered.

The ionization energy and the electronic affinity were linked to the energies of the HOMO and LUMO orbitals as follows [15]:

$$I = -E_{HOMO} \qquad (3)$$

$$A = -E_{LUMO} \qquad (4)$$

The global electronegativity (χ) and the chemical hardness (ή) and of a chemical system are expressed

by the following equations:

$$\chi = \frac{I + A}{2} = -\mu \qquad (5)$$

$$\acute{\eta} = \frac{I - A}{2} \qquad (6)$$

The softness (S), which is the inverse of the global hardness, is given as:

$$S = \frac{1}{\acute{\eta}} = \frac{2}{I - A} \qquad (7)$$

The electrophilicity index (ω) was calculated using the following equation [16]:

$$\omega = \frac{\chi^2}{2\acute{\eta}} \qquad (8)$$

The fraction of electrons (ΔN), transferable from the inhibitor molecule to the metallic surface was calculated using the following equation [17]:

$$\Delta N = \frac{\phi - \chi_{inh}}{2(\acute{\eta}_{Al} + \acute{\eta}_{inh})} \qquad (9)$$

where ϕ and η_{Al} signify the work function and absolute hardness of Al mainly accepted as 4.28 eV and 0, respectively; χ_{inh} and $\acute{\eta}_{inh}$ represent the electronegativity and hardness of the inhibitor, respectively. The nucleophilic (f_k^+) and electrophilc (f_k^-) Fukui functions as well as the dual descriptor (Δf) were predicted on the basis of the finite difference approximation as follows [18]:

$$f_k^+ = q_k(N + 1) - q_k(N) \qquad (10)$$

$$f_k^- = q_k(N) - q_k(N - 1) \qquad (11)$$

$$\Delta f(k) = f_k^+ - f_k^- \qquad (12)$$

where q_k denotes the electronic population of an atomic site within a molecule in its anionic (N + 1), neutral (N), or cationic (N − 1) state.

2.4. Molecular dynamics simulation

The simulation of adsorption of 5-ATT molecule on Al surface was done using Forcite module of the Materials Studio package. Drawing tools in visualized materials are employed to construct 5-ATT molecule as well as aluminium surface. The Al (1 1 0) plane being the greatest stable surface was adopted to represent the metallic substrate. The interplay between 5-ATT and Al surface was assumed in a simulation box (29.99 Å × 25.26 Å × 27.68 Å) with periodic border conditions. An adequate vacuum region of 40.00 Å was used to avert the possible intersupercell interactions that can be caused by the periodic border condition. In acidic solution, the -NH_2 group of 5-ATT have a great tendency to be protonated. Thus, the protonated 5-ATT molecule was engaged in the simulation. Moreover, the spatial

position of aluminium atoms in Al (110) were kept fixed, and the surface plane was loaded with water molecules (400), chloride (23), hydronium ions (24) along with a protonated inhibitor molecule. The simulation was carried out at 303.0 K under the COMPASS force field and the NVE ensemble using time step of 1.0 fs and simulation time of 500 ps. The interaction energy $E_{Al\text{-}inhibitor}$ between the 5-ATT molecule and the Al (110) surface was estimated according to the following equation [19]:

$$E_{Al-inhibitor} = E_{Total} - (E_{Al+solution} + E_{inhibior}) \quad (13)$$

where E_{Total} denotes the total energy of the full system; $E_{Al+solution}$ signifies the total energy of the Al (110) and solution without an inhibitor molecule, $E_{inhibitor}$ represents the total energy of free inhibitor molecule. The binding energy was the negative sign value of interaction energy as follows:

$$E_{binding} = -E_{Al-inhibitor} \quad (14)$$

2.5. Surface examination studies

For surface morphological studies using SEM, the cleaned aluminium specimens (2.5 cm x 2.5 cm x 0.3 cm) were examined before and after 6 h immersion in 1 M HCl blank solution, and inhibited solution with 2.0 mM of 5-ATT at 308 K. After 6 h, the specimens were retrieved, cleaned appropriately and then dried at room temperature. The morphology of all samples was observed via SEM instrument (PRO: X: Phenonm World 800-07334) operating at an accelerating voltage of 15 kV, and images were obtained at 500× magnification.

3. Results and discussion

3.1. Weight loss analysis

3.1.1. Effect of inhibitor concentration

The experimental data of corrosion rate and inhibition efficiency for aluminium in 1 M HCl in the absence and presence of different concentrations of 5-ATT at 308 K are disclosed in **Table 1.** It is evident from this Table that on increasing the concentration of 5-ATT inhibitor, the corrosion rate decreased and thus, reflecting an increase in inhibition efficiency. This implies that on increasing the concentration, inhibitor molecules are adsorbed on the aluminium surface to the greater extent by providing a wider surface coverage. Consequently, a barrier film is formed which restricts the interaction between the metal and the corrosive solution. Thus, the maximum inhibition performance of 93.72% was obtained when the test solution was pretreated with 2.0 mM of the inhibitor. The corrosion suppression ability of the 5-ATT molecule can be attributed to the presence of lone pair of electrons on the heteroatoms (N and S) as well as the π-electron system in it structure which synergistically increased the electron density at adsorption sites on the molecule, thereby enhanced its adsorption proficiency and hence increased its

corrosion inhibition performance [20].

Table 1. Corrosion parameters obtained for aluminium in 1 M HCl containing different concentrations of 5-ATT at 308 K.

Conc. (mM)	C_R (mg. cm^{-2} h^{-1})	IE (%)
Blank	7.65	–
0.1	3.71	51.50
0.5	1.61	78.95
1.0	1.03	86.53
1.5	0.67	91.24
2.0	0.48	93.72

3.1.2. Effect of immersion time

The results of weight loss analysis performed in 1 M HCl in the presence of 2.0 mM 5-ATT inhibitor for varying immersion time at 308 K are presented in **Table 2.** The results clearly demonstrate that the corrosion rate decreases and the inhibition efficiency increases by prolonging the immersion time. The increase in inhibition efficiency with increasing time may be ascribed to the restriction of access of the corrosive agent to the metal surface by the accumulated corrosion products. Similar trend was reported elsewhere [12].

Table 2. Variation of C_R and IE with immersion time for aluminium corrosion in 1 M HCl in the absence and presence of 2.0 mM concentration of 5-ATT at 308 K.

Time (h)	C_R (mg. cm^{-2} h^{-1})	IE (%)
3	0.88	89.28
6	0.48	91.59
9	0.36	93.36
12	0.31	94.28

3.1.3. Effect of Temperature

Temperature is one of the key factors that influence the corrosion phenomenon of metallic materials. The most of complexes formed during inhibition process can readily dissolve when temperature increase, which results in an appreciable decrease in the anticorrosion properties of molecules employed in the inhibition of metals corrosion. In order to determinate the stability of the tested inhibitor, weight loss measurements have been carried out in uninhibited and inhibited test solution at 308 K, 318 K, 328 K and 338 K. The results reported in **Table 3** show that the values of corrosion rate in the absence and

presence of 5-ATT increase clearly with rising temperature. However, the inhibition efficiency decreases with the increase in temperature of the corrosive medium. The decrease in inhibition efficiency with temperature was essentially due to the desorption of inhibitor molecules at the elevated temperatures [21].

Table 3. Corrosion parameters obtained for aluminium in 1 M HCl containing different concentrations of 5-ATT at varying temperatures.

Conc. (mM)	C_R (mg. cm^{-2} h^{-1})				IE (%)			
	308 K	318 K	328 K	338 K	308 K	318 K	328 K	338 K
Blank	7.65	9.40	13.3	17.4	—	—	—	—
0.1	3.71	5.12	7.98	10.76	51.50	45.53	40.00	38.16
0.5	1.61	2.58	3.75	5.01	78.95	72.55	71.80	70.20
1.0	1.03	1.61	2.39	3.32	86.53	82.87	81.03	80.90
1.5	0.67	0.98	1.70	2.38	91.24	89.57	87.21	86.32
2.0	0.48	0.79	1.21	1.75	93.72	91.59	90.90	89.94

The Arrhenius and transition state equations have been employed to express the temperature dependence of the corrosion rate. This is expressed using the following equations [22]:

$$\log C_R = \frac{-E_a}{2.303RT} + \log A \qquad (15)$$

$$\log\left(\frac{C_R}{T}\right) = \left[\log\left(\frac{R}{Nh}\right) + \frac{\Delta S_a^*}{2.303\ R}\right] - \frac{\Delta H_a^*}{2.303\ RT} \qquad (16)$$

where, E_a signifies the activation energy; T is absolute temperature; R is the gas constant (8.314 J mol^{-1} K^{-1}); A is the Arrhenius pre-exponential factor; N is Avogadro's number; h is Planck's constant, ΔS* and ΔH* are the entropy and enthalpy of activation, respectively.

Fig. 2 illustrates the Arrhenius and transition state plots for dissolution of aluminium in 1 M HCl in the absence and presence of different concentration of 5-ATT. The values of E_a were obtained from the gradients of straight lines in **Fig. 2a.** The values of ΔS* and ΔH* were also determined from the intercept and gradient of straight lines in **Fig. 2b**, respectively. The values of the corresponding extracted parameters are listed in **Table 4**.

The estimated activation energies for the inhibited solutions were found to be higher in comparison to the uninhibited solution. The higher values of Ea for inhibited solution correspond to the increase in the energy barrier for metallic dissolution process in the presence of inhibitor molecules [23]. Besides, the positive values of activation enthalpy (ΔH*) reflected the endothermic behavior, resulting in a slow process of metal dissolution. The values of the activation entropy (ΔS*) displayed in **Table 4** decreases

less negatively with the presence of the 5-ATT inhibitor. This signify the formation of a stable layer of this inhibitor on the aluminium surface. Meanwhile, the negative sign of ΔS* implies that the activated complex represents an association rather than a step of dissociation, which suggest a decrease in disorder on transition from reactant to the activated complex [21,22].

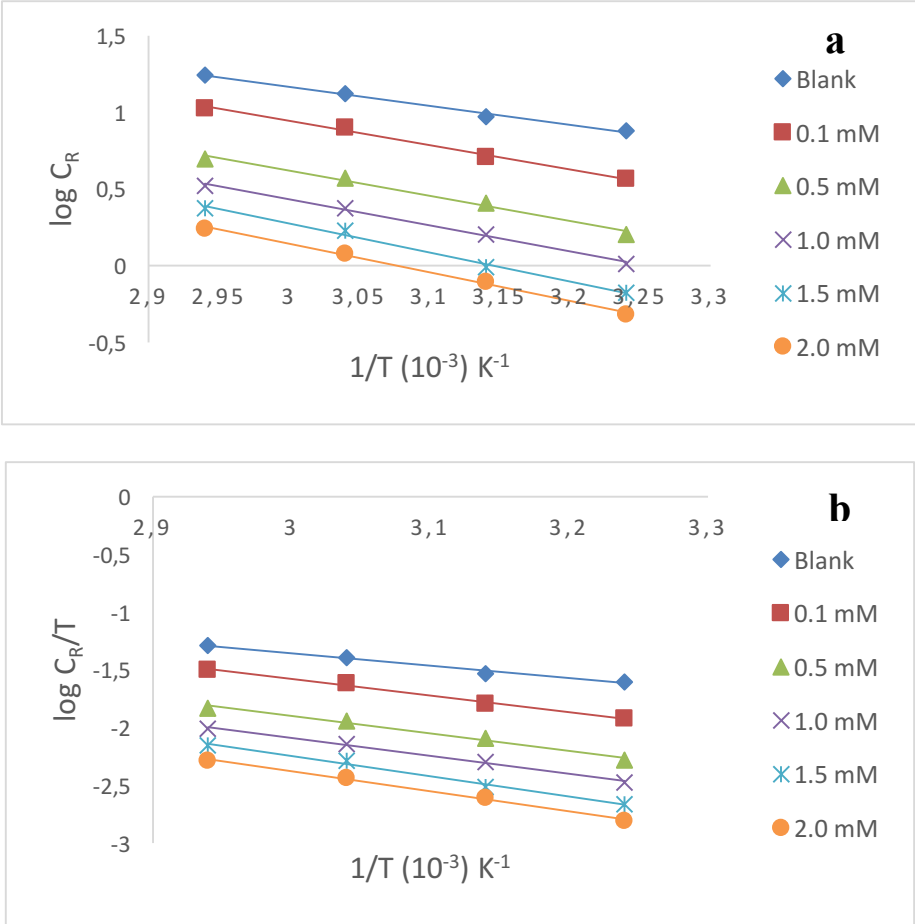

Fig. 2. (a) Arrhenius and (b) transition state plots for aluminium corrosion in 1 M HCl in the absence and presence of different concentration of 5-ATT.

Table 4. Activation parameters for dissolution of aluminium in 1 M HCl in the absence and presence of different concentration of 5-ATT.

C_{inh} (mM)	E_a (kJ mol^{-1})	A (mg cm^{-2})	ΔH^* (kJ mol^{-1})	ΔS^* (J mol^{-1} K^{-1})
0.0	23.77	7.8 x 10^4	20.54	-181.96
0.1	30.17	2.6 x 10^5	27.80	-174.51
0.5	32.42	3.5 x 10^5	28.78	-173.76
1.0	33.26	3.6 x 10^5	29.91	-172.85
1.5	36.25	5.5 x 10^5	30.69	-172.22
2.0	37.00	9.1 x 10^5	33.25	-170.57

3.2. Adsorption isotherm and thermodynamic considerations

The adsorption of inhibitors on the metal surface has been established as the first step in the corrosion inhibition process and is regarded as a substitution reaction between the organic inhibitor molecules in the aqueous phase and water molecules adsorbed on the metal surface [24]:

$$OI_{(aq)} + n\,H_2O_{(ads)} \rightarrow OI_{(ads)} + n\,H_2O_{(aq)} \qquad (17)$$

where, $OI_{(aq)}$ and $OI_{(ads)}$ denote the organic inhibitor molecules that exist in solution and in adsorbed form on the metal surface, respectively, and the size ratio which signifies the number of water molecules replaced by one molecule of organic adsorbate, is denoted as n.

Adsorption isotherm provides crucial insight about the interaction between the inhibitor molecules and metal surface. The inhibitors can adsorbed on a corroding metal surface either physically or chemically, where the molecules physisorbed slow metal dissolution by inhibiting the cathodic reaction while chemisorbed molecules inhibit the anodic reaction by reducing the reactivity of the metal at adsorption sites [25]. Thus, the adsorption mechanism depend on the electronic structure of inhibitor molecule, nature of metal surface and the electrolyte type [20]. In this study, several adsorption isotherms including Langmuir, Temkin, Frumkin and Flory-Huggins have been employed to elucidate the adsorption behavior of 5-ATT on the aluminium surface. The Langmuir adsorption isotherm exhibited the best fit to the experimental data which is defined by the following equation [26]:

$$\frac{C}{\Theta} = \frac{1}{K_{ads}} + C \qquad (18)$$

where K_{ads} is the adsorptive equilibrium constant; C is the concentration of inhibitor and Θ is the surface coverage which can be calculated as per eq. 19:

$$\Theta = \frac{C_R^0 - C_R^i}{C_R^o} \qquad (19)$$

where C_R^o and C_R^i denote the corrosion rate in the absence and presence of 5-ATT inhibitor, respectively. The plots of C/Θ against C **(Fig. 3)** obtained at varying temperature yielded straight lines ($R^2 > 0.99$), indicating that adsorption of 5-ATT on aluminium surface obeys Langmuir isotherm more accurately compared to other isotherms. The adsorption energy ΔG^o_{ads} is a key thermodynamic parameter which is linked to the adsorptive equilibrium constant (K_{ads}) based on the following equation [22]:

$$\Delta G^0_{ads} = -RT\ln(55.5\,K_{ads}) \qquad (20)$$

where R is the universal gas constant and T is the absolute temperature. The constant value of 55.5 represents the molar concentration of water in solution. The changes in standard adsorption enthalpy (ΔH^o_{ads}) and entropy (ΔS^o_{ads}) can be determined using the fundamental thermodynamic equation:

$$\Delta G^o_{ads} = \Delta H^o_{ads} - T\Delta S^0_{ads} \qquad (21)$$

The values of ΔS^{o}_{ads} and ΔH^{o}_{ads} were estimated from the gradient and intercept of the plot of ΔG^{o}_{ads} versus T presented in **Fig. 4**. The extracted thermodynamic parameters are collected in **Table 5**. Generally, the high values of K_{ads} inferred the strong adsorption of the 5-ATT on the aluminium surface, and subsequently a superior inhibition behavior [27]. It is observed also that K_{ads} values decreases with rising temperature, signifying that the interactions between the adsorbed molecules and the aluminium surface are weakened and, consequently, the adsorbed molecules become easily removable. The negative values of ΔG^{o}_{ads} affirm that the 5-ATT was adsorbed spontaneously on the metal surface. Prosaically, ΔG^{o}_{ads} values up to −20 kJ mol^{-1} are compatible with the electrostatic interactions between the charged inhibitor molecules and charged metal surface (physical adsorption), while those more negative than −40 kJ mol^{-1} involve charge transfer or sharing from the inhibitor molecules to the vacant d-orbitals of the metal surface to form a coordinate covalent bond (chemical adsorption) [28,29]. In the current study, the calculated values of ΔG^{o}_{ads} range from −33.86 to −32.08 kJ mol^{-1}, suggesting that the adsorption of 5-ATT on the metal surface might involve a combination of both physisorption and chemisorption mechanisms [21,30]. From the results in **Table 5**, the value of ΔH^{o}_{ads} is negative which reflects the exothermic nature of the adsorption process. In general, an exothermic process is mostly attributed to either physisorption or chemisorption, while endothermic adsorption process infer chemisorption [31]. The positive value of ΔS^{o}_{ads} implies that the adsorption process is accompanied by entropy increase, which is ascribed to water molecules displacement from the metal surface by inhibitor molecules [12,13]. Altogether, the results reflect the mixed physicochemical character of the adsorption of the 5-ATT molecules onto the metal surface.

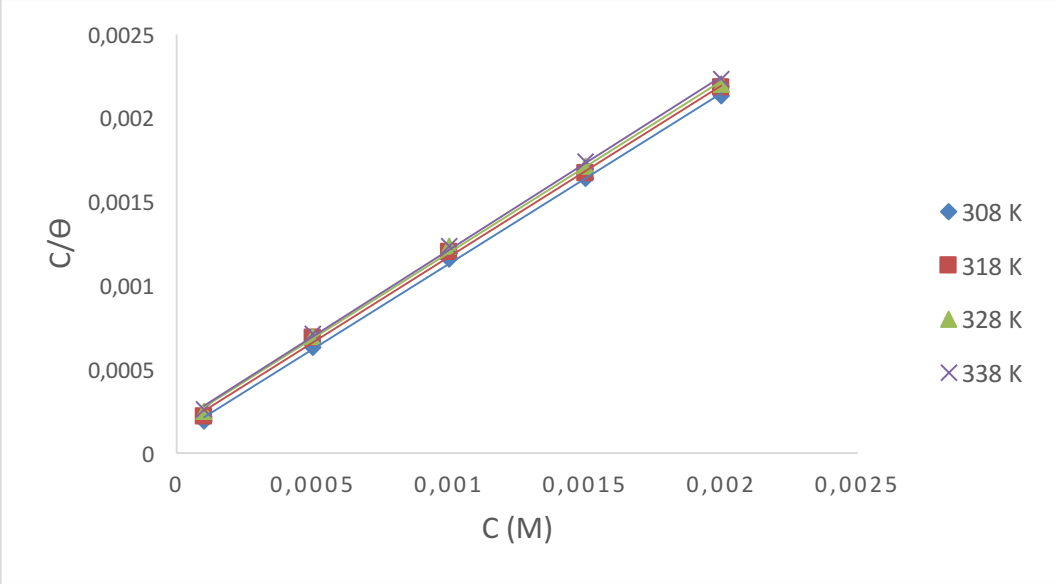

Fig. 3. Langmuir's isotherm plots for adsorption of 5-ATT on aluminium surface in 1 M HCl

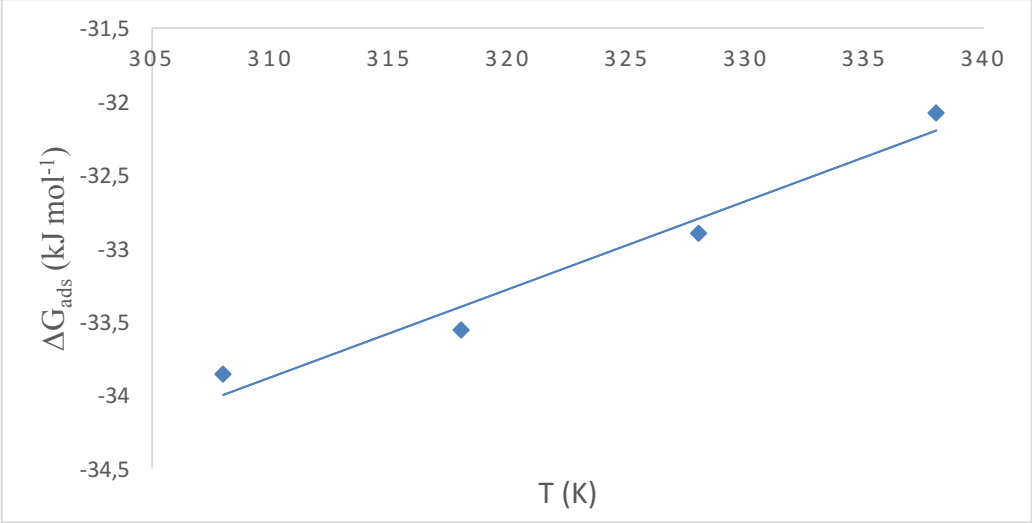

Fig. 4. Plot of ΔG^{o}_{ads} versus T for estimation of thermodynamic parameters

Table 5. Thermodynamic adsorption parameters of 5-ATT on aluminium in 1 M HCl at different temperatures.

T (K)	K_{ads} (x 10^3 M)	ΔH^{o}_{ads} (kJ mol^{-1})	ΔS^{o}_{ads} (J $mol^{-1}K^{-1}$)	ΔG^{o}_{ads} (kJ mol^{-1})
308	10.00	−54.66	67.40	−33.86
318	5.88			−33.56
328	4.98			−32.16
338	4.76			−32.08

3.3. Quantum chemical calculations

3.3.1. Global reactivity descriptors

Quantum chemical calculations using the B3LYP/DND level of theory were undertaken to gain insight about the geometric and electronic properties of the 5-ATT. Optimized molecular structure and Frontier molecular orbital's density distribution obtained are depicted in **Fig. 5.** It is clear from the **Fig. 5**, that the isodensity in HOMO and LUMO of 5-ATT is evenly distributed throughout the entire molecular structure of the inhibitor molecule, suggesting a parallel adsorption onto metal surface. This could result in enhanced adsorption of the inhibitor on the aluminium surface through dual interactions, that is, interactions between the unshared electron pair of heteroatoms and the unoccupied d-orbitals of metal atoms. The computed quantum chemical parameters are shown in **Table 6.** The ionization potential corresponds to the HOMO energy and thus demonstrates the susceptibility of an inhibitor molecule to donate an electron [30]. Higher HOMO energy potentially leads to a higher electron donating ability, whereas the LUMO energy corresponds to the electron affinity and portrays the propensity of the molecule to accept electron [32].

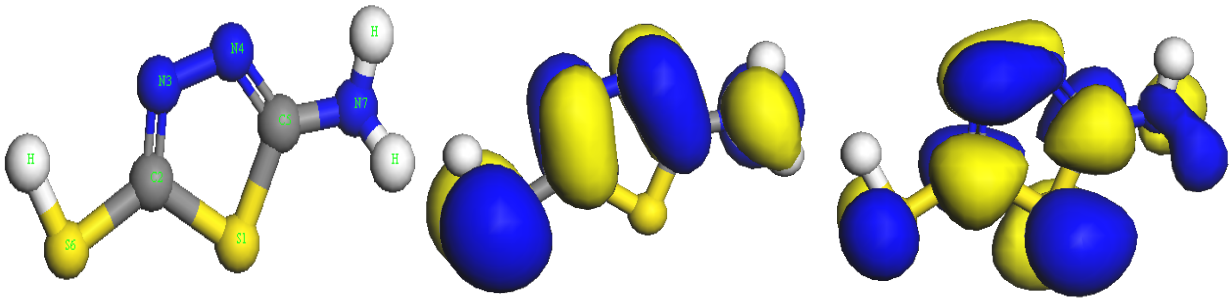

Fig. 5. Optimized molecular structure (left), HOMO (center) and LUMO (right) distribution for 5-ATT

In our case, 5-ATT has a high value of HOMO energy (−4.752 eV) and a low value of LUMO energy (−1.084 eV). It has been reported that good corrosion inhibitors are usually those compounds that can play the dual roles; donating electrons to vacant orbital of the metal and acquiring free electrons from the metal surface [25]. Thus, the incompletely filled 3p orbital in aluminium could interact with the HOMO of 5-ATT whereas the filled 3s orbital could bond with its LUMO [22].

The donor−acceptor interactions can also be measured by the number of transferred electrons from the corrosion inhibitors to the metal surface. The positive ΔN value (0.743) reflect the greater tendency of the inhibitor molecule to share its electrons with the metal surface [32]. The energy gap (ΔE) is a key parameter for diagnosing chemical reactivity and stability of inhibitor molecule. The lower value of ΔE (3.668 eV) shows that 5-ATT is reactive and can be adsorbed easily on aluminium surface, because less excitation energy is needed to remove electrons from the last occupied orbital. The electrophilicity index (ω) is another crucial parameter which measures the capability of chemical species to acquire electrons; a high value of electrophilicity index signifies a strong electrophile while a small value of electrophilicity implies a strong nucleophile [33]. In this study, ω = 2.321 eV indicates that 5-ATT has a great capacity to accept electrons from the aluminium.

Table 6. Calculated quantum chemical parameters for 5-ATT at the B3LYP/DND level of theory

E_{HOMO} (eV)	E_{HOMO} (eV)	ΔE (eV)	I (eV)	A (eV)	χ (eV)	ή (eV)	S (eV)	ώ (eV)	ΔN
−4.752	−1.084	3.668	4.572	1.094	2.918	1.834	0.545	2.321	0.743

3.3.2. Local Reactivity

In order to predict the active sites on the inhibitor molecule on which nucleophilic and electrophilic reactions are likely to occur, the 5-ATT molecule was studied by the condensed Fukui function analysis. The favored site for nucleophilic attack is the atom which has the highest value of f_k^+ while the preferred site for electrophilic attack is located on atom which has the highest value of f_k^- [25]. The condensed

Fukui functions of 5-ATT were computed by applying Mulliken and Hirshfeld population analysis, which is disclosed in **Table 7**. As shown in **Table 7,** S1 and S6 are the most reactive sites for nucleophilic attack. Similarly, the value of f_k^- is highest on the same atoms which shows that they are also the preferred sites for an electrophilic attack. The observed similarity in the sites for nucleophilic and electrophilic suggests similarity in mechanism of inhibition [34].

Table 7. The Fukui functions of 5-ATT (excluding H atoms) calculated at the B3LYP/DND level of theory

Atom	Mulliken		Hirshfield	
	f_k^+	f_k^-	f_k^+	f_k^-
S1	**0.247**	0.159	**0.226**	0.126
C2	0.079	0.015	0.102	0.058
N3	0.096	0.094	0.107	0.098
N4	0.070	0.103	0.083	0.106
C5	0.085	0.046	0.091	0.065
S6	0.183	**0.296**	0.177	**0.286**
N7	0.044	0.100	0.072	0.115

3.4. Molecular dynamics simulation

Molecular dynamics (MD) simulation has been conducted to get further insight about the interaction between 5-ATT and Al (1 1 0) surface. The optimized equilibrium configuration of the investigated inhibitor molecule (both top and side views) are displayed in **Fig. 6** and the calculated energies are shown in **Table 8.** By inspecting the result presented in **Fig. 6**, it can be observed that the inhibitor molecule can approach the target surface in a nearly flat or parallel orientation. Actually, the flat orientation can maximize contact area between inhibitor molecule and aluminium substrate making an obstruction between the metal surface and aggressive particles and thus protecting it from corrosion. Meanwhile, the extent of adsorption of an inhibitor molecule on the metal substrate may be predicted using the interaction and binding energies. Higher interaction/binding energy basically shows better adsorption of an inhibitor molecule on aluminium surface. Interestingly, the data presented in **Table 8** revealed that the value of interaction energy of the simulation system was large and negative, implying that the adsorption 5-ATT on Al (1 1 0) surface is strong and spontaneous [35]. Moreover, the magnitude of the binding energy (66.935 kcal mol^{-1}) between Al (1 1 0) surface and inhibitor molecule was less than 100 kcal mol^{-1} intimating that the adsorption occurred through mixed physisorption and chemisorption mechanism [36].

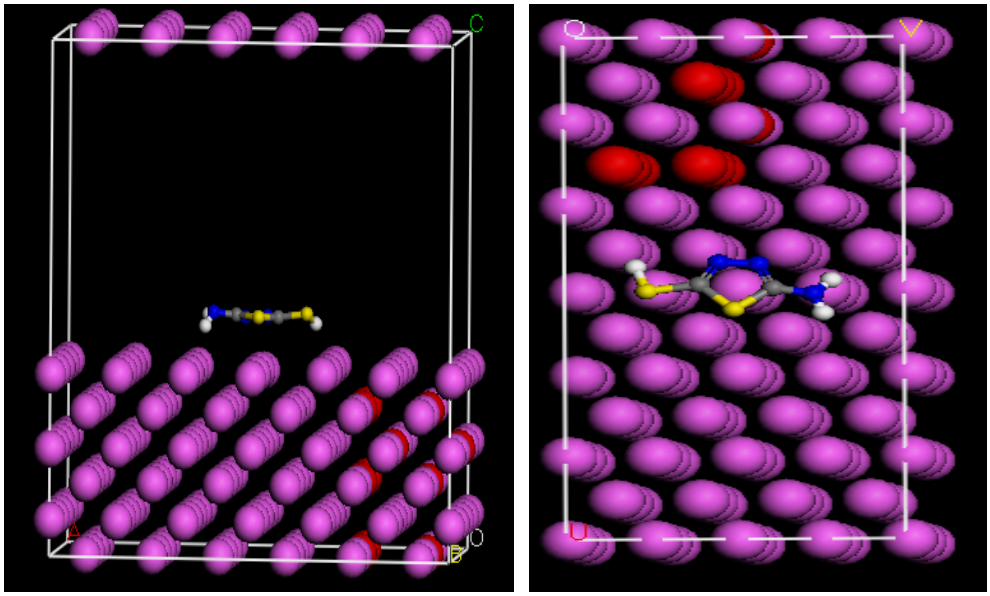

Fig. 6. Equilibrium configurations of 5-ATT adsorbed on Al (1 1 0) surface, side and top view.

Table 8. MD parameters for the 5-ATT adsorbed on Al (110) surface

Properties (kcal mol^{-1})	Values
Total energy	−104.028
Inhibitor energy	−37.093
Al (110) surface energy	0.000
Interaction energy	−66.935
Binding energy	66.935

3.5. Surface analysis

SEM images displaying the polished, corroded and inhibited aluminum surfaces are presented in **Fig. 7**. After immersion in the blank 1 M HCl solution for 6 h, the aluminum surface was damaged, as can be observed in **Fig. 7(b).** The corroded layer of the specimen is rather rough and cracked due to the destructive attack of HCl solution. In contrast, the aluminium surface remained intact appreciably by the presence of 5-ATT inhibitor **(Fig. 7c),** signifying suppression in the corrosion phenomenon. Moreover, the smoother texture of aluminium specimen exposed to inhibited acid solution demonstrates improvement in the surface morphology which could be ascribed to the blocking of active centers on the metal surface by the inhibitor molecules. These observations verify that the anticorrosive activity of 5-ATT is based on the formation of protective film at the metal surface, which protect the aluminium against the corrosive medium.

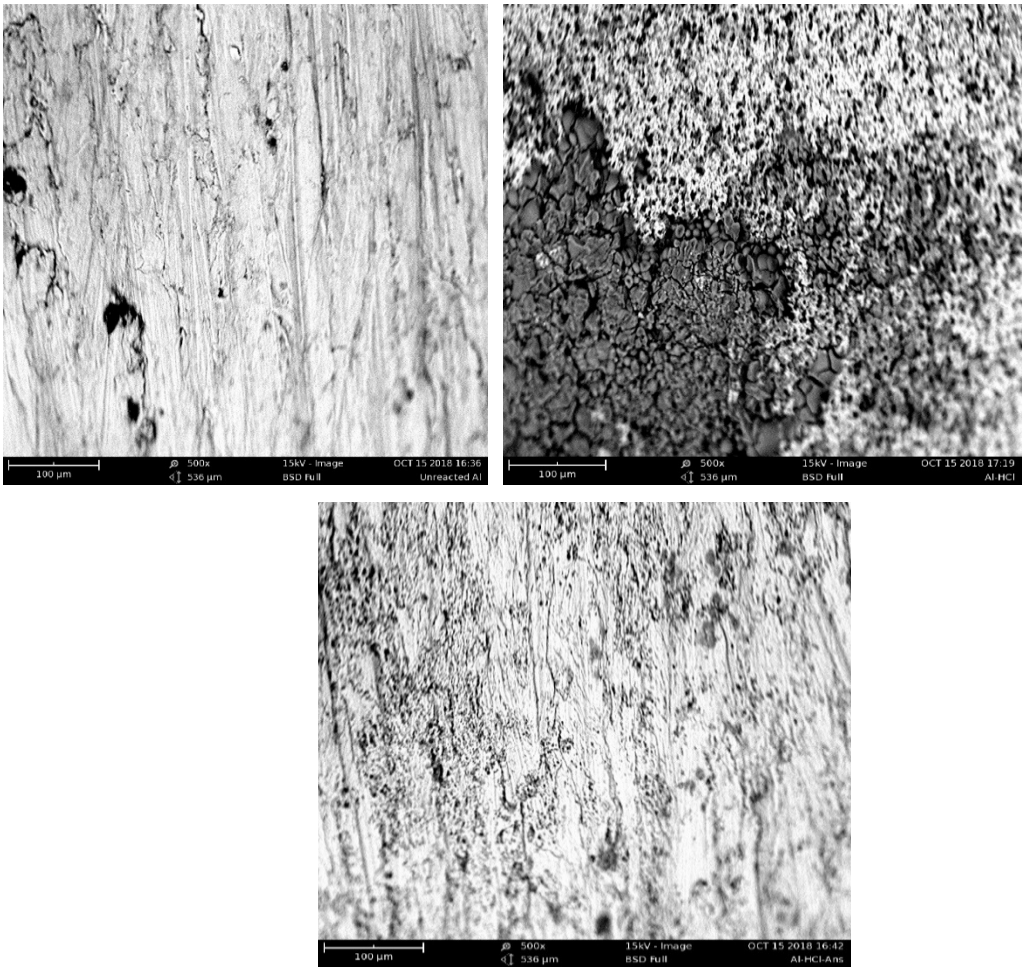

Fig. 7. SEM images of the aluminum surface in the absence and presence of 5-ATT inhibitor: (a) polished surface (b) corroded surface (c) inhibited surface

Conclusion

The inhibition efficiency of 5-ATT on aluminium corrosion in 1 M HCl was evaluated using weight loss measurements, quantum chemical calculations, molecular dynamics method and SEM technique. From the findings of our investigation, it is safe to conclude that:

1. The inhibition efficiency increases with increasing 5-ATT concentration and immersion time but decreased with rise in temperature.
2. The adsorption of target 5-ATT inhibitor on aluminium surface follows the Langmuir isotherm.
3. The thermodynamic analysis revealed that the 5-ATT molecules interact with the metal substrate via mixed physichemisorption mechanism.
4. Electronic structure parameters and inhibition efficiency of the investigated compound was correlated with the help of quantum chemical calculations.
5. The computational simulations showed that the studied inhibitor was adsorbed strongly on the aluminium surface in a parallel orientation, which can minimize metal surface area attacked by corrosive media.

6. Surface analysis using SEM reflected an appreciable mitigation of aluminium corrosion by the formation of protective film of inhibitor on the metal surface.
7. Overall, the investigated 5-ATT proved to be effective corrosion inhibitor for aluminium in 1 M HCl medium.

Conflict of Interest: The authors declare that the research was conducted in the absence of any commercial or financial relationships that could be construed as a potential conflict of interest.

References

[1] H. J. Grahke, Corrosion et chimie de surfaces des métaux. *Materials and Corrosion*, 45: 146–146 (1994)

[2] K. S. Rao and K. P. Rao, Corrosion Resistance of AA2219 Aluminium Alloy: Electrochemical Polarisation and Impedance Study. *Mater. Sci. Technol*. 22, 1: 97–104 (2006).

[3] N. D. Alexopoulos, C. J. Dalakouras, P. Skarvelis, S. K. Kourkoulis, Accelerated corrosion exposure in ultra-thin sheets of 2024 aircraft aluminium alloy for GLARE applications. *Corros. Sci*. 55: 289–300 (2012).

[4] M. H. Hussin, M. J. Kassim, N. Razali, N. Dahon, and D. Nasshorudin, The effect of *Tinospora crispa* extracts as a natural mild steel corrosion inhibitor in 1 M HCl solution. *Arabian J. Chem*. 9: S616–S624 (2016).

[5] J. C. D. Rocha, J. A. D. C. P. Gomes, E. D'Elia, Aqueous extracts of mango and orange peel as green inhibitors for carbon steel in hydrochloric acid solution. *Mater Res*. 17: 1581-1587 (2014).

[6] A. Aytaç, Cu(II), Co(II) and Ni(II) Complexes of –Br and –OCH2CH3 Substituted Schiff Bases as Corrosion Inhibitors for Aluminium in Acidic Media. *J. Mater. Sci.* 45, 24: 6812–6818 (2010).

[7] C. Verma, P. Singh, I. Bahadur, E. E. Ebenso, M. A. Quraishi, Electrochemical, thermodynamic, surface and theoretical investigation of 2-aminobenzene-1,3-dicarbonitriles as green corrosion inhibitor for aluminum in 0.5M NaOH. *J Mol. Liq.* 209: 767–778 (2015).

[8] T. Zhang, W. Jiang, H. Wang and S. Zhang, Synthesis and Localized Inhibition Behaviour of New Triazine-Methionine Corrosion Inhibitor in 1 M HCl for 2024-T3 Aluminium Alloy. *Mater. Chem. Phys.* 237: 121866 (2019).

[9] A. S. Yaro, A. A. Khadom and R. K. Wael, Apricot juice as green corrosion inhibitor of mild steel in phosphoric acid. *Alexandria Eng. J.* 52: 129–135 (2014).

[10] C. Kamal, and M. G. Sethuraman, *Spirulina platensis*—A novel green inhibitor for acid corrosion of mild steel. *Arabian J. Chem.* 5: 155–161 (2012).

[11] B. Xu, Y. Ji, X. Zhang, X. Jin, W. Yang and Y. Chen, Experimental and theoretical studies on the corrosion inhibition performance of 4-amino-N,N-di-(2-pyridylmethyl)aniline on mild steel in

hydrochloric acid. *RSC Adv.* 5: 56049 (2015).

[12] H. Ouicia, M. Tourabib, O. Benalic, C. Sellesd, C. Jamae, A. Zarroukf, F. Bentissb, Adsorption and corrosion inhibition properties of 5-amino 1,3,4-thiadiazole- 2-thiol on the mild steel in hydrochloric acid medium: Thermodynamic, surface and electrochemical studies. *J. Electroanalytical Chem*. 803: 125–134 (2017).

[13] M. Guzmán, R. Lara and L. Vera, 5-Amino-1,3,4-Thiadiazole-2-Thiol Corrosion Current Density and Adsorption Thermodynamics on Astm A-890-1b Stainless Steel in A 3.5% Nacl Solution. *J. Chil. Chem. Soc*. 54: 2 (2009).

[14] M. Husaini, U. Yunusa, H. A. Ibrahim, B. Usman, and M. B. Ibrahim, Corrosion inhibition of aluminium in phosphoric acid solution using glutaraldehyde as inhibitor. *Alg. J. Chem. Eng*. 1: 12-21 (2020).

[15] C. C. Zhan, J. A. Nichols, D. A. Dixon, Electron affinity, electronegativity, hardness, and electron excitation energy: molecular properties from density functional theory orbital energies. *J Phys. Chem. A*. 107: 4184-4195 (2003).

[16] S. Liu, R. G. Parr, Consequences for exchange energy density functional of exponentially decaying nature of atomic electron densities. *J Comput. Chem*. 20: 2-11 (1999).

[17] R. G. Pearson, Hard and soft acids and bases-the evolution of a chemical concept. *Coordination Chem. Rev.* 100: 403–425 (1990).

[18] H. Mi, G. Xiao, X. Chen, Theoretical Evaluation of Corrosion Inhibition Performance of Three Antipyrine Compounds. *Comput.. Theor. Chem*. 1072: 7−14 (2015).

[19] U. Yunusa, S.A. Idriss, Y.L. Muhammad, A. Hudu, T. Abdullahi and U. Umar, *Jatropha podagrica* stem bark extract as a novel green corrosion inhibitor for carbon steel in acid medium: A combined experimental and computational explorations. *Applied Journal of Environmental Engineering Science.* 7: 241-260 (2021).

[20] C. Verma, L. O. Olasunkanmi, E. E. Ebenso, M. A. Quraishi, Adsorption characteristics of green 5-arylaminomethylene pyrimidine- 2,4,6-triones on mild steel surface in acidic medium: Experimental and computational approach. *Results in Physics* 8: 657–670 (2018).

[21] M. Chadili, M. M. Rguiti, B. El Ibrahimi, Corrosion Inhibition of 3003 Aluminum Alloy in Molar Hydrochloric Acid Solution by Olive Oil Mill Liquid By-Product. *Int. J. Corrosion*. 6662395, (2021).

[22] R. H. B. Beda, P. M. Niamien, E. B. Avo Bilé, and A. Trokourey, Inhibition of Aluminium Corrosion in 1.0M HCl by Caffeine: Experimental and DFT Studies. *Adv. Chem*. 6975248, (2017).

[23] M. Yadav, S. Kumar, R. R. Sinha, S. Kumar, Experimental and Theoretical Studies on Synthesized

Compounds as Corrosion Inhibitor for Mild Steel in Hydrochloric Acid Solution. *J. Dispersion Sci. Technol.* 35: 1751−1763 (2014).

[24] I. R. Burrows, K. L. Dick, J. A. Harrison, A comparison of the rate of copper deposition at mercury, copper amalgam and copper metal. *Electrochim Acta*. 21: 81–84 (1976).

[25] A. S. Fouda, M. A. Ismail, A. S. Abousalem and G. Y. Elewady, Experimental and theoretical studies on corrosion inhibition of 4-amidinophenyl-2,20-bifuran and its analogues in acidic media. *RSC Adv.* 7, 46414 (2017).

[26] L. O. Olasunkanmi, I. B. Obot and E. E. Ebenso, *RSC Adv*. 6: 86782–86797 (2016).

[27] H. Gerengi, H. I. Sahin, *Schinopsis lorentzii* extract as a green corrosion inhibitor for low carbon steel in 1 M HCl solution. *Ind*. *Eng*. *Chem*. *Res*. 51: 780– 787 (2012).

[28 A. I. Adawy, M. A. Abbas, K. Zakaria, *Res*. *Chem*. *Intermed*. 42: 3385 (2016).

[29] C. M. Goulart, A. Esteves-Souza, C. A. Martinez-Huitle, C. J. F. Rodrigues, M. A. M. Maciel, A. Echevarria. Experimental and theoretical evaluation of semicarbazones and thiosemicarbazones as organic corrosion inhibitors. *Corros*. *Sci.* 67: 281–91 (2013).

[30] B. Chugh, A. K. Singh, S, Thakur, Comparative Investigation of Corrosion-Mitigating Behavior of Thiadiazole-Derived Bis-Schiff Bases for Mild Steel in Acid Medium: Experimental, Theoretical, and Surface Study. *ACS Omega*. 5: 13503−13520 (2020).

[31] C. Verma, P. Singh, I. Bahadur, E. E. Ebenso and M. A. Quraishi, *J*. *Mol*. *Liq*. 209, 767–778 (2015).

[32] U. Nazir, Z. Akhter, N. Z. Alib and F. U. Shah, Experimental and theoretical insights into the corrosion inhibition activity of novel Schiff bases for aluminum alloy in acidic medium. *RSC Adv*. 9: 36455 (2019).

[33] J. Saranya, P. Sounthari, K. Parameswari, and S.Chitra, Adsorption and density functional theory on corrosion ofmild steel by a quinoxaline derivative. *Der Pharma Chemica*. 7, 8: 187–196 (2015).

[34] I. Danaee, F, S. RameshKumar, M. RashvandAvei*c*, M. Vijayan**,** Electrochemical and Quantum Chemical Studies on Corrosion Inhibition Performance of 2,2'-(2-Hydroxyethylimino)bis[N-(alphaalpha-dimethylphenethyl)-N-methylacetamide] on Mild Steel Corrosion in 1M HCl Solution. *Mater. Res*. 23, 2: e20180610 (2020).

[35] Z. Yavari, M. Darijani, M. Dehdab, Comparative Theoretical and Experimental Studies on Corrosion Inhibition of Aluminum in Acidic Media by the Antibiotics Drugs. *Iran J Sci Technol Trans Sci.* (2017).

[36] C. O. Akalezi, C. K. Enenebaku, E. E. Oguzie, Application of aqueous extracts of coffee senna for control of mild steel corrosion in acidic environments. *Int*. *J*. *Ind*. *Chem*. 3, 1: 13 (2012).